Synaptic Integration in Electrically Coupled Neurons

Elizabeth García-Pérez,* Mariana Vargas-Caballero,* Norma Velazquez-Ulloa,* Antonmaria Minzoni,† and Francisco F. De-Miguel*
*Departamento de Biofísica, Instituto de Fisiología Celular, and †FENOMEC (IIMAS), UNAM, 04510 D.F., México

ABSTRACT Interactions among chemical and electrical synapses regulate the patterns of electrical activity of vertebrate and invertebrate neurons. In this investigation we studied how electrical coupling influences the integration of excitatory postsynaptic potentials (EPSPs). Pairs of Retzius neurons of the leech are coupled by a nonrectifying electrical synapse by which chemically induced synaptic currents flow from one neuron to the other. Results from electrophysiology and modeling suggest that chemical synaptic inputs are located on the coupled neurites, at 7.5 μm from the electrical synapses. We also showed that the space constant of the coupled neurites was 100 μm, approximately twice their length, allowing the efficient spread of synaptic currents all along both coupled neurites. Based on this cytoarchitecture, our main finding was that the degree of electrical coupling modulates the amplitude of EPSPs in the driving neurite by regulating the leak of synaptic current to the coupled neurite, so that the amplitude of EPSPs in the driving neurite was proportional to the value of the coupling resistance. In contrast, synaptic currents arriving at the coupled neurite through the electrical synapse produced EPSPs of constant amplitude. This was because the coupling resistance value had inverse effects on the amount of current arriving and on the impedance of the neurite. We propose that by modulating the amplitude of EPSPs, electrical synapses could regulate the firing frequency of neurons.

INTRODUCTION

Electrical synapses couple the electrical activity of neurons in central and peripheral nervous systems of vertebrates and invertebrates (Bennett et al., 1963; Auerbach and Bennett, 1969; Baker and Llinás, 1971; Llinás et al., 1974; Nicholls and Purves, 1972; Korn et al., 1973; Schmalbruch and Jahnsen, 1981; McMahon, 1994). Interactions of chemical and electrical synapses synchronize the activity of groups of neurons, from invertebrate (Marder and Eisen, 1984; Rela and Szczupak, 2003) to mammalian central neurons (Galarreta and Hestrin, 1999, 2001; Gibson et al., 1999; Tamas et al., 2000; Szabadics et al., 2001). The co-localization of chemical and electrical synapses in dendrites offers the possibility that the flow of synaptic currents across the electrical synapse may reduce the amplitude of the chemically induced synaptic responses in the driving dendrite, in proportion to the degree of electrical coupling. Another effect would be the spread of the chemically induced synaptic responses to the coupled dendrite, which, by receiving these inputs, extends its effective dendritic tree.

We analyzed these possibilities in pairs of electrically coupled Retzius neurons of the Mexican leech *Haementeria officinalis*. Each of the 21 segmental ganglia of this species contains nearly 325 neurons distributed in a stereotyped manner (E. Izquierdo, and F. F. De-Miguel, unpublished). Retzius neurons are the largest in each ganglion and release serotonin from presynaptic endings (Henderson, 1983) and from the soma (Trueta et al., 2003), by which they modulate swimming (Willard, 1981; Nusbaum and Kristan, 1986), local bending (Kristan, 1982; Lockery and Kristan, 1990), and learning (Burrel et al., 2001). The pair of Retzius neurons in each segmental ganglion is coupled by a nonrectifying electrical synapse (Hagiwara and Morita, 1962; Eckert, 1963), which is presumably formed between neurites arising from the primary axon (Lent, 1973; Mason and Leake, 1978; De-Miguel et al., 2001). In addition, both Retzius neurons receive a common chemical synaptic input (Hagiwara and Morita, 1962) which produces EPSPs that spread to the other neuron through the electrical synapse (De-Miguel et al., 2001).

To explore how electrical coupling affects the integration of EPSPs, we measured morphological and biophysical parameters of Retzius neurons to design a mathematical model that reproduced their electrical responses. The model was combined with experimental evidence to calculate the location of the presynaptic chemical inputs onto the neurites, the space constant of the neurites, and the coupling resistance value. We also made quantitative simulations as to how chemically induced synaptic currents produced by such inputs are distributed in both coupled neurites. As our main finding we show that the leak of synaptic currents from one neuron to another may determine the amplitude of the EPSPs in the driving neurite.

MATERIALS AND METHODS

Preparation

Experiments were carried out in isolated ganglia of adult leeches *H. officinalis*, at room temperature (20–25°C). Intersegmental ganglia were dissected out and pinned in Sylgard-coated dishes containing leech Ringer fluid composed of (mM): NaCl, 115; KCl, 4; $CaCl_2$, 1.8; glucose, 11; Tris maleate 10 buffered to pH 7.4 (J.T.Baker D.F., Mexico). Ganglion capsules were extremely hard and resisted cell impalements by microelectrodes. For this reason, the capsules were opened with forceps, and the somata of

Submitted June 26, 2003, and accepted for publication August 19, 2003.

Address reprint requests to Dr. Francisco F. De-Miguel, Dept. de Biofísica, Instituto de Fisiología Celular, UNAM, Apartado Postal 70-253, 04510 D.F., México. Tel.: 525-622-5622; Fax: 525-622-5607; E-mail: ffernand@ifisiol.unam.mx.

0006-3495/04/01/646/10 $2.00

Retzius neurons were exposed to the bathing fluid. The somata of Retzius neurons could be unequivocally identified by their characteristic size and position in the ganglion.

Electrophysiological techniques

Intracellular recordings were made with borosilicate glass microelectrodes (FHC, Bowdoinham, ME) and were filled with 3 M KCl. Their tip resistances ranged from18 to 25 MΩ. The microelectrodes were coupled to preamplifiers (Almost Perfect Electronics, Basel, Switzerland), and recordings were filtered by a custom-designed Bessel filter with a cutoff frequency of 400 Hz. Data were acquired by an analog-to-digital board Digidata 1200 (Axon Instruments, Foster City, CA) using Axoscope 8.0 or Pclamp 8.0 and stored in a PC for further analysis.

For current injection, we used an independent microelectrode. This was preferred over single-electrode current clamp in switch-mode because of the need to inject large amounts of current. A constraint of this method was the possible somatic ''shunt'' produced by each microelectrode. However, after five minutes of recording, the membrane sealed around the electrode tip, allowing accurate estimates of the membrane properties (Fig. 4). Artificial synaptic potentials similar to natural EPSPs were produced by injecting 300–500 μs depolarizing current pulses into one of the neurons. The amount of current was adjusted to produce voltage amplitudes of 1–2 mV. The membrane time constant defined the decay phase of the artificial EPSP (Fig. 6).

The coupling coefficient was defined as V_2/V_1, where V_1 is the voltage of the driving neuron (in which current was injected, or in which a synaptic potential was produced), and V_2 is the voltage of the coupled neuron. Therefore, the coupling coefficient was defined as V_2/V_1. For recordings of spontaneous activity this nomenclature was used arbitrarily.

Morphology

The morphology of Retzius neurons was studied by double staining of pairs of neurons. We injected lucifer yellow (LY) into one neuron and Texas Red (TR) or horseradish peroxidase (HRP) (LY, TR, and HRP, Sigma, St. Louis, MO) into the other neuron. None of these dyes cross through the electrical synapse (Muller and McMahan, 1976; Stewart, 1978; De-Miguel et al., 2001). HRP injections were made following the procedure of Muller and McMahan (1976). The rest of the procedure was performed as described by Macagno et al. (1981). Pairs of fluorescent neurons were imaged in serial z series taken at 1.0 μm intervals under calibrated confocal optics (Bio-Rad, Hemel Hempstead, UK) using fluorescein and rhodamine emission wavelengths and a Nikon X40 oil immersion objective.

The quantitative analysis of the neurite length and diameter, and of the number of sites of contact of pairs of neurons was made from deconvolved (X-Cosm free software; http://ibc.wustl.edu/bcl/xcosm/xcosm.html; Biomedical Computer Laboratory,Washington University, St. Louis, MO) confocal z series, taken using a Nikon X100 oil immersion objective (NA 1.25). Calibration of confocal images and the choice of the number of iterations of the deconvolution process were made using yellow-green– or red-fluorescent carboxylate-modified microspheres of 2.0 and 0.5 μm diameter (FluoSpheres, Molecular Probes, Eugene, OR; Fig. 2). Measurements were made manually using Confocal Assistant 4.02 (Bio-Rad) and Metamorph Imaging System 3.6 software (Universal Imaging, West Chester, PA).

Cell culture

The membrane time constant of the soma was measured from neurons that were isolated and kept in culture. The isolation procedure was slightly different from the original one (Dietzel, et al. 1986; Trueta et al., 2003) in that L-15 culture medium (Gibco, D.F., Mexico) was diluted in leech Ringer solution (1:1). To obtain spherical somata without processes, the treatment with 2 mg/ml collagenase/dispase (Boehringer-Mannheim, Darmstadt, Germany) lasted only 25–30 min. After the enzyme treatment, the somata of Retzius neurons were sucked out one by one and sterilized by rinsing them several times in culture solution. Neurons were plated in plastic culture dishes coated with concanavalin A (Sigma). To restrict neurite outgrowth, neurons were plated with their stumps pointing upward. In these conditions the neurons survived for more than a week and kept their resting potentials between −50 and −55 mV. The low density of sodium channels in the soma of Retzius neurons (García, et al., 1990) made it hard for them to produce action potentials in response to injection of positive current pulses. However, neurons that retained their excitability were excluded from our analysis.

Electron microscopy

Cultured neurons were washed with 0.08 M cacodylate buffer (Sigma) and fixed for 10 min with 0.6% glutaraldehyde (Sigma) and 0.4% paraformaldehyde in 0.08 M cacodylate buffer, pH 7.4. Postfixation was made with 1% osmium tetroxide (Fluka, St. Louis, MO) in cacodylate buffer. Thin sections were counterstained with uranyl acetate for 10 min and with lead citrate for 2.5 min. Observations were made in a Jeol 1010 electron microscope (Jeol USA, Peabody, MA). Measurements of the membrane perimeter were made from digitized images using Metamorph Imaging System 3.6 software (Universal Imaging).

Modeling

A model of electrically coupled Retzius neurons was designed using linear cable theory applied to circuits representing the somata linked with neurites. A detailed description of the model and the mathematics used for this design are in Appendix 1 of the Supplementary Material. The strategy for designing the model was based on our own morphological evidence and on the approach of Yang and Chapman (1983). We considered the cell soma as a circuit with parallel capacitance and resistance, the neurites as finite cables with electrotonic length $L = \ell/\lambda$, and the electrical synapse as a coupling resistance (r_c) connecting neurites of both Retzius neurons (Fig. 2). The parameters used in the model are defined in Table 1. Simulations of chemically induced synaptic currents were made assuming that inputs were established onto single electrically coupled neurites. It is also noteworthy that electrically coupled neurites were in parallel (Fig. 3); therefore, when current was injected into the soma of one neuron, all of the neurites displayed the same voltage changes.

The transfer function of the model was obtained by using Laplace transforms (Jack et al., 1975; see Supplemental Material). The values of the coupling resistance and the space constant of the neurites were estimated by fitting the transfer function of the model to experimental data (see Fig. 4) using least-square estimates. The dependence of the EPSP rise time and amplitude on the location of the presynaptic inputs along the neurites was analyzed by using the saddle point method (Jack et al., 1975). To test the accuracy of our model, the predicted shapes of EPSPs at the cell somata were compared with artificial EPSPs produced by current injection into the soma of one neuron.

RESULTS

Synaptic activity of Retzius neurons

During simultaneous recordings from pairs of Retzius neurons, EPSPs arrived in synchrony (less than 5 ms in between) at the soma of both neurons (Fig. 1, *A* and *B*), supporting the idea of a common presynaptic chemical input onto both coupled neurons (Hagiwara and Morita, 1962; De-Miguel et al., 2001). EPSPs were classified into two populations according to their rise times. Seventy-nine percent

TABLE 1 Definition of symbols and values estimated and used in the model

Symbol	Definition (dimension)	Soma	Neurites
C_s	Specific membrane capacitance of the soma (μF/cm^2)	1	—
c_s	Capacitance of the soma (μF)		
D	Diameter (μm)	60–80	1.08
ℓ	Cable length (μm)	—	50
λ	Space constant (μm)	—	100
$L = \ell/\lambda$	Electrotonic length	—	0.50
r_a	Axial resistance $r_a = 4\ell R_a/\pi d^2$ (GΩ/cm)	—	85–1273
r_c	Coupling resistance (MΩ)	—	30–340
R_s	Specific membrane resistance of the soma (Ωcm^2)	18–40	—
r_s	Membrane resistance of the soma (MΩ)	90–150	—
τ	Membrane time constant of the soma $\tau = r_m c_m = R_m C_m$ (ms)	18–40	—
T	Rise time of EPSPs (ms); peak 1 peak 2	5.6 ± 0.24; 9.6 ± 0.33	
V_1	Voltage response of the driving cell (mV)		
V_2	Voltage response of the follower cell (mV)		
X	Distance between the somata (μm)		

of the pairs of synchronous EPSPs had similar (5.6 ± 0.24 ms; $n = 11$ neurons) rise times in both neurons, suggesting that they were produced by a chemical input common to both neurons. The amplitudes of these EPSPs varied between both neurons and from one EPSP to the next in the same neuron, presumably because of presynaptic fluctuations in the amount of transmitter being released (Fig. 1C_1; De-Miguel et al., 2001). The EPSPs of the second population had slower (9.6 ± 0.33 ms) rise times and were always paired with a fast EPSP in the coupled neuron. The proportion of slow EPSPs was increased from 21% to 40% by reducing the presynaptic release probability with an external solution containing 1 mM Ca^{2+} and 2 mM Mg^{2+}. Since this manipulation reduced the average amplitude of the EPSPs without changing their kinetics, we conclude that the slow EPSPs were produced by an input onto the coupled neuron and that they were detected due to a local transmission failure (Fig. 1C_2; De-Miguel et al., 2001). Accordingly, the rise time distribution of EPSPs was bimodal (Fig. 7 *B*), supporting the idea that the EPSP populations were produced by an input onto each of the coupled neurons. Action potentials were produced in either neuron from the summation of both types of EPSPs (Fig.1 *D*), and in every case they were followed by another action potential in the coupled neuron after a lag of several milliseconds.

Model design

Since the site of EPSP initiation was not accessible for recordings, we developed a model as a complementary tool to analyze the spread of EPSPs. The model was based on the morphology and passive electrical properties of the neurons. We estimated experimentally the time constant, the resistance and capacitance of the soma, as well as the length and the geometry of the neurites.

The morphology of 17 pairs of neurons filled with intracellular dyes was similar to those previously described

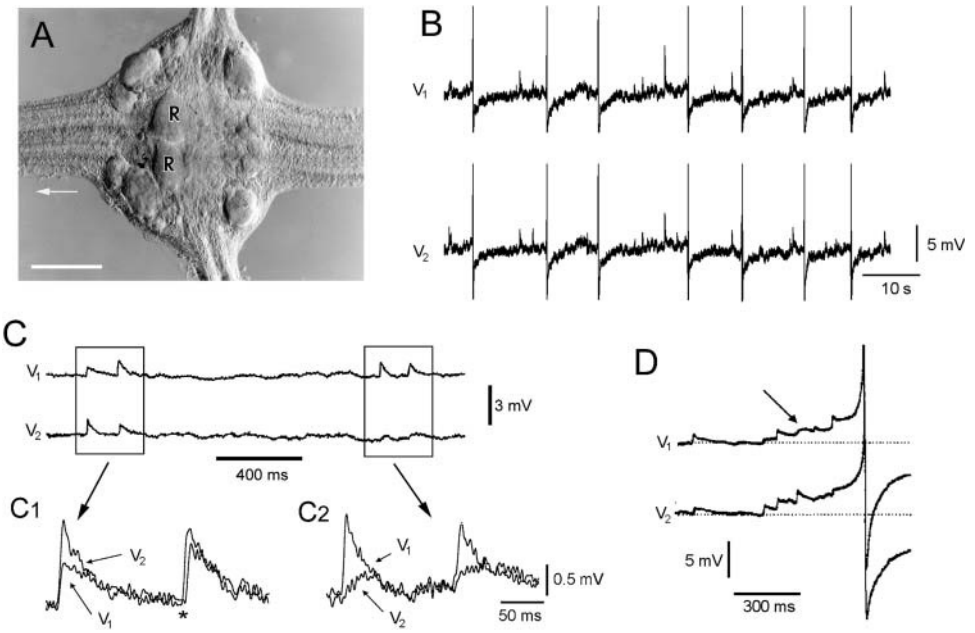

FIGURE 1 Electrical activity of Retzius neurons. (*A*) Nomarski image of a leech ganglion showing the somata of the pair of electrically coupled Retzius neurons (*R*). Arrow points anterior. Scale bar = 100 μm. (*B*) Simultaneous recordings from both Retzius neurons in one ganglion. V_1 and V_2 are the voltage recordings from each neuron. Synchronous action potentials (*large truncated spikes*) and EPSPs (*small spikes*) composed the spontaneous electrical activity pattern of these neurons. (*C*) Superposition of pairs of EPSPs recorded simultaneously from both neurons. The EPSPs boxed are amplified in C_1 and C_2. (C_1) The amplitudes of EPSPs varied from one EPSP to the next and from one neuron to the other, although their rise and decay times were similar, suggesting presynaptic variations of transmitter release. (C_2) Upon transmission failures onto either of the neurons, EPSPs produced in the other neuron could be recorded from both somata. EPSPs arriving from the coupled neuron (marked as V_2) were slower and were also attenuated in amplitude. (*D*) Action potentials were produced by summation of EPSPs produced locally with those arriving from the coupled neuron (*arrow*). The following EPSPs produced an action potential in V_1 (*truncated spike*), which was followed by another action potential in the coupled neuron.

(Lent, 1973; Mason and Leake, 1978; De-Miguel et al., 2001). Both neurons in each ganglion were a mirror image of each other. The 60–80 μm soma was connected to a primary axon from which multiple neurites were sent in all directions. Branches of the primary axon traveled out of the ganglion through the connective nerves and through the nerve roots (Fig. 2 *A*).

In seven pairs of neurons studied by double staining, the contact sites were formed by neurites sent to the central region of the neuropile (Fig. 2; De-Miguel et al., 2001). The length of this population of neurites was 49.93 $\pm$ 5.7 μm (n = 90 neurites). After the deconvolution process to the z series of images, we found that neurites making contact had constant diameters with an average value of 1.08 $\pm$ 0.03 μm.

Most of the 45.4 $\pm$ 2.6 contact sites were at the tips of the neurites and had the same diameter (Fig. 2 *B*); thus, for modeling purposes, we considered that the contact sites did not contribute to the capacitance of the circuit. As seen by comparing the responses of the model and neurons shown in Figs. 5 and 6, this was a good approximation. Our measurements were within the linear range of resolution of our optical system, as shown by the calibration with fluorescent beads of 0.5 and 2.0 μm and emission wavelengths in the rhodamine and fluorescein ranges (Fig. 2 *C*), similar to those of the fluorescent dyes injected into the neurons. Fig. 2 *D* shows a partial reconstruction of a neurone with the region of neurites making contact surrounded by the red lines. In three neurons, the percentage of neurites without branches making contact with the coupled neuron was 71%, 76%, and 63%, respectively (n = 204 neurites). The rest of the neurites making contact (n = 59; discontinuous lines in Fig. 2 *D*) had one (91%) or more (9%) branches, all of which had the same diameter as the mother neurites, thus failing to follow the 3/2 power rule for an electrotonically equivalent cable (Rall, 1959). The distribution of the contact sites in the arborization of a Retzius neuron is shown in Fig. 2 *E*. Note that most of the contact sites were established by neurites proximal to the soma.

Based on this morphology, we modeled the neuronal somata as circuits with parallel resistance (r_s) and capacitance (c_s) (Fig. 3) coupled directly to the neurites. The large axons were included in our original version of the model, although they were excluded from the rest of the analysis since, as shown by Yang and Chapman (1983), they did not have a significant contribution to the somatic coupling, presumably because they are isopotential with the soma (Ross et al., 1987). The large proportion of nonbranched neurites making contact allowed us to model the whole population as homogeneous cables with length ℓ = 50 μm and space constant λ. The electrotonic distance of the neurites was defined as the ℓ/λ coefficient (Fig. 3). The cables from each neuron were coupled by a resistor (r_c). Note that with this configuration, artificial or simulated synaptic potentials produced at one soma would give the same voltage changes along all of the coupled neurites, as they are connected in parallel.

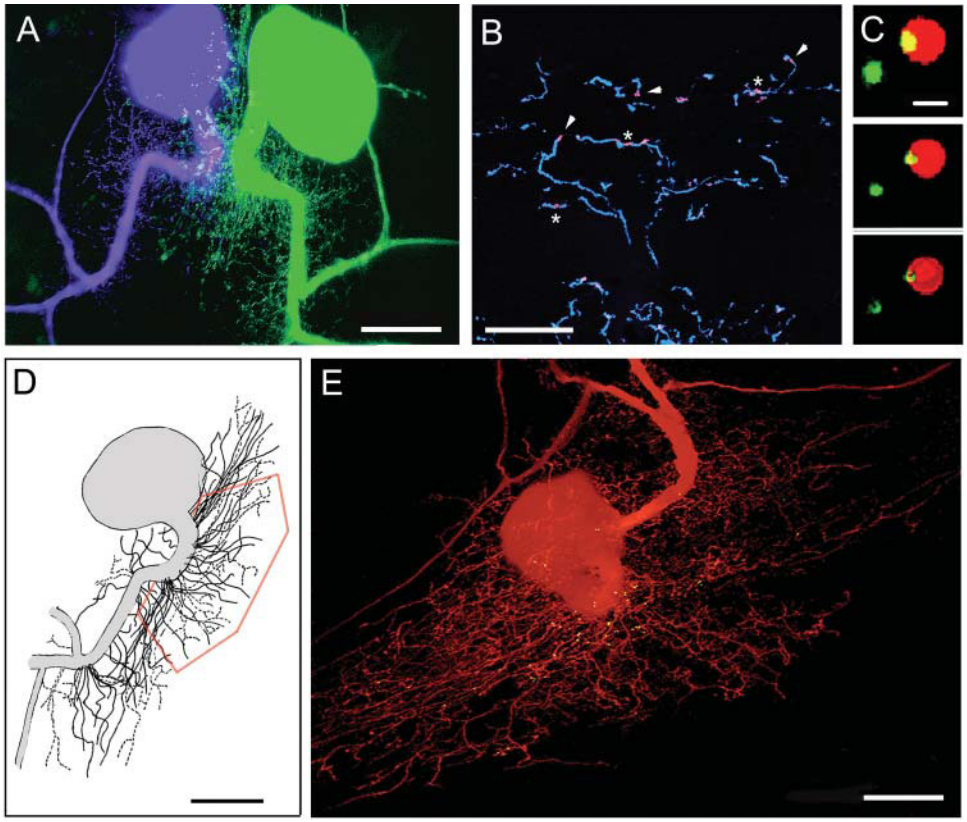

FIGURE 2 Morphology of Retzius neurons. (*A*) Three-dimensional confocal reconstruction of a pair of Retzius neurons. The green neuron was filled with Texas red, and the purple neuron was filled with lucifer yellow. Images were not deconvolved. Scale = 40 μm. (*B*) Deconvolved partial (10 μm depth) reconstruction of the arborization of a Retzius neuron (*blue*). The contact sites are digitally superimposed (*pink*). Scale = 15 μm. (*C*) Confocal images of fluorescent beads of 0.5 (*green*) and 2.0 (*red*) μm diameters. Image on top was before deconvolution. The images in the middle and bottom were deconvolved with 20 and 50 iterations, respectively. Scale = 2.0 μm. (*D*) Partial reconstruction of a Retzius neuron. The area of contact is surrounded by the red lines. Neurites without branches are the continuous lines, and neurites with branches are the dotted lines. Scale = 40 μm. (*E*) Reconstruction of a Retzius neuron from confocal z series of deconvolved images. The yellow spots are contact sites digitally superimposed. Note that contact sites were restricted to an area proximal to the soma. Scale = 40 μm.

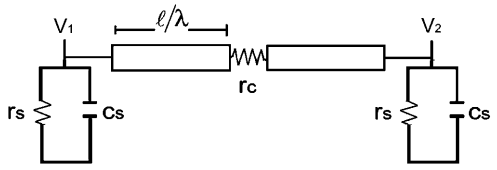

FIGURE 3 Electrical model of a pair of Retzius neurons. The somata, which were isopotential with the large primary axons, are represented as circuits with parallel resistance (r_s) and capacitance (c_s). Each soma is connected to neurites, one of which is represented as a finite cable of length ℓ and space constant λ. The electrotonic distance of the neurites is defined as ℓ/λ. Neurites from both neurons are connected by a coupling resistance (r_c).

Electrical parameters of the soma

The contribution of the soma to EPSP integration was determined by its impedance, $Z_{soma} = r_s/1 + j\varpi\tau$ (see the Supplementary Material, in which the intrinsic parameters were r_s (the soma membrane resistance) and τ (the time constant; Table 1; see Supplementary Material). Both parameters were measured from somata that were isolated and kept in culture (Fig. 4 *A*) where they maintained their resting potential values similar to those of neurons in the ganglion.

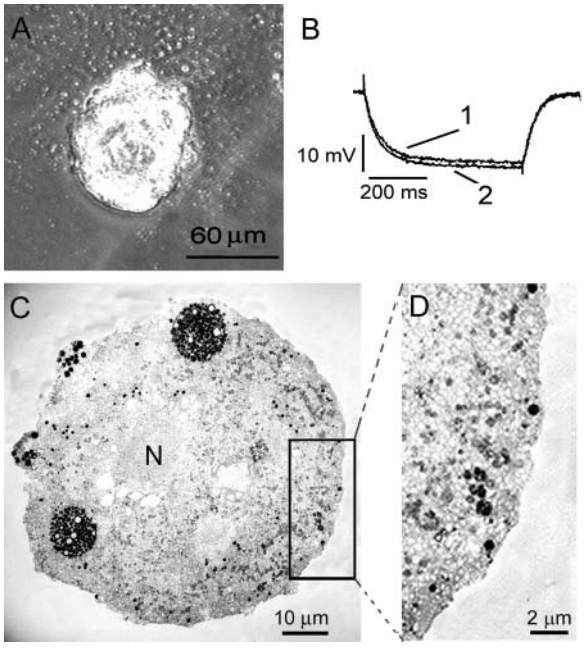

FIGURE 4 Estimates of the somatic time constant and membrane area. (*A*) Phase contrast image of the soma of a Retzius neuron in culture. (*B*) The time constant of neurons in culture was measured from the exponential decay time of the voltage response to the injection of square hyperpolarizing current pulses. The time constant was similar before (1) and after (2) a second electrode had impaled the neuron, showing that the soma ''shunt'' effect was minimal. The artifacts in trace 1 are due to bridge balance and show the beginning and end of the current pulse. (*C*) Electron micrograph of the soma of a Retzius neuron in culture showing invaginations of the plasma membrane. The nucleus (*N*) can also be seen. (*D*) Higher magnification of the region boxed in *C*.

A τ value of 20.8 ± 3.4 ms (ranging from 18 to 40 ms) was obtained from exponential fits to the steady-state voltage responses at the end of square hyperpolarizing current pulses of 500 ms (Fig. 4 *B*) in 12 neurons maintained at −60 mV by the injection of negative DC current. The soma shunt produced by the microelectrode was minimal, since the values of τ before and 5 min after the insertion of a second electrode were similar (Fig. 4 *B*), showing that the cell membrane sealed around the electrode. Therefore, we assumed that our estimates gave an accurate approximation to the real value of τ. Data from neurons that failed to recover after the second impalement were excluded from our analysis.

The values of the membrane resistance (r_s), were obtained from the formula $r_s = \tau/(\text{soma surface area})$ (C_s), where C_s is the specific membrane capacitance (1 μF/cm^2). Since the membrane infoldings could have a significant contribution to the surface area, estimates of this parameter were made from electron micrographs (Fig. 4, *C* and *D*). The amount of infolding of these neurons was similar to that of neurons in the ganglion (V. H. Hernandez, M. Morales, and F. F. De-Miguel, unpublished). The radius obtained from the real perimeters were used to calculate the total surface area, assuming that the neurons were spherical. In eight neurons, the areas obtained by this method ranged between 1.13×10^{-4} and 3.14×10^{-4} cm^2, and were 25% larger than those calculated from images obtained under phase contrast optics. The corresponding values of r_s were between 90 and150 MΩ (Table 1).

Sinusoidal domain responses of neurons and model

To test the accuracy of the model and the values of the parameters estimated above (Table 1), we studied the frequency responses to injection of sine wave currents of six pairs of neurons with steady-state coupling ratios between 0.26 and 0.63. These responses were compared with model simulations (Fig. 5; Eq. 14 of the Supplementary Material). The model predictions compared well with the frequency responses of every pair of neurons and were similar to the responses of a first-order, low-pass filter, demonstrating that the system operated linearly. The best fits of the experimental data with the model predictions in every pair of neurons were obtained when $\lambda = 100$ μm, that is, twice the individual neurite length (50 μm; ℓ/λ ratio of 0.5), but similar to the distance between both somata. This low ℓ/λ coefficient guaranteed an efficient EPSP conduction along the neurites.

The r_c values calculated ranged from 30 MΩ when the coupling ratio was 0.72, to 340 MΩ when the coupling ratio was 0.22. Two extreme conditions of the model (Yang and Chapman, 1983) failed to fit with our data. If λ is infinite, a fair representation of the circuit is with both somata bound directly by r_c (Fig. 5 *C*, *left inset*). The second condition occurred when the r_c value is so low that both somata are coupled by a continuous cable (Fig. 5 *C*, *right inset*).

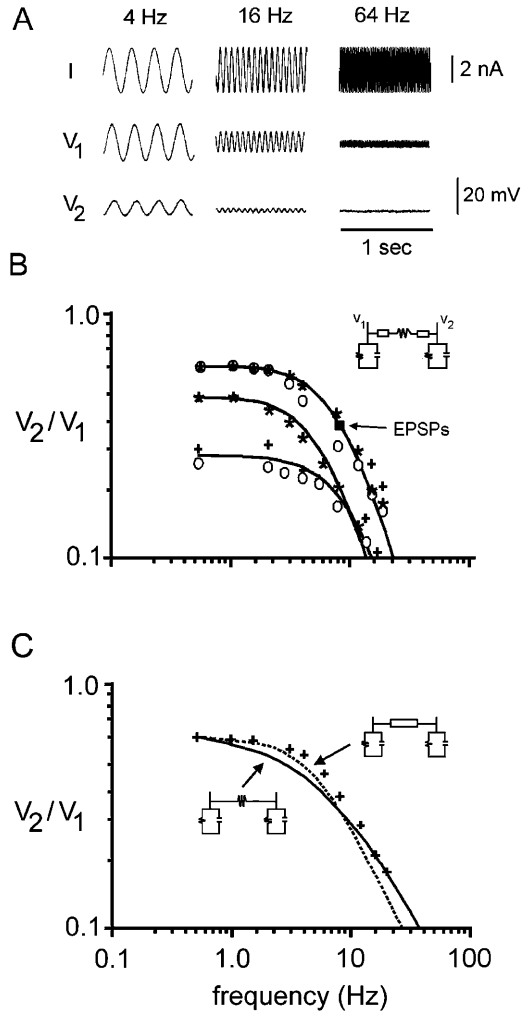

FIGURE 5 Frequency responses of neurons and model. (*A*) Sine wave currents (*I*) of different frequencies (*top traces*) injected into the soma of a Retzius neuron and voltage responses in the driving (V_1) and coupled (V_2) neurons. The amplitude and phase shift of the voltage responses of both neurons were frequency dependent. (*B*) Responses of six pairs of neurons with steady-state coupling ratios between 0.62 and 0.26 are presented with different symbols. The continuous lines are best fits of these responses with the predictions of the model shown in the inset. The parameter values used are in Table 1. (*C*) The two extreme conditions of the model shown in the insets failed to fit with the experimental data.

To show the effect of λ and r_c on the spread of EPSPs along the neurites, the shape and amplitude of artificial EPSPs at both somata were compared with model simulations. Fig. 5 shows an example in which the steady-state coupling ratio was 0.35. The amplitude of the simulated EPSPs was fixed at V_1, and the r_c values were changed between 15 (below the value estimated for this coupling ratio) and 80 MΩ (Fig. 6). When the ℓ/λ coefficient was fixed at 0.5 and the r_c value at 30 MΩ, the shape of the simulated responses reproduced that of artificial EPSPs. As expected, changing the r_c value produced an inversely proportional change in the amplitude of the EPSP at V_2 without affecting its kinetics.

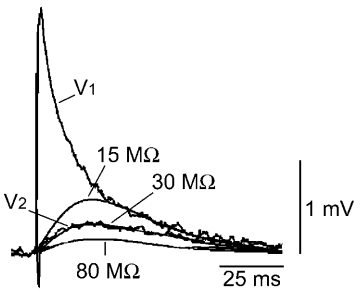

FIGURE 6 Effect of coupling resistance in the spread of EPSPs. Computer simulations reproduced the spread of artificial EPSPs from the soma of the driving neuron (V_1) to the soma of the coupled neuron (V_2) . Changing the coupling resistance value in the simulations from 15 to 30 and 80 MΩ modified the amplitude but not the shape of the EPSPs in V_2.

Location of presynaptic inputs in the coupled neurites

To estimate the location of presynaptic chemical inputs, we compared the somatic coupling ratio of natural and artificial EPSPs (Fig. 6). Owing to the passive properties of the neurites, a chemical input located right beside the electrical synapse should produce the largest somatic EPSP coupling ratio. This ratio should decrease as the input is more proximal to the soma. For this reason, the coupling ratio of EPSPs produced in the coupled neurites should be larger than that of artificial EPSPs produced at the soma. On the other extreme, the coupling ratio of EPSPs produced in noncoupled neurites should be smaller than that of artificial EPSPs.

In seven pairs of neurons the coupling ratio of artificial EPSPs was smaller than that of natural EPSPs, as expected for inputs located in the coupled neurites. Fig. 7 *A* superimposes natural and artificial EPSPs from a pair of neurons with a steady-state coupling ratio of 0.56. The amplitudes were normalized for comparison of their kinetics. In this representative pair of neurons, the coupling ratio of 10 averaged artificial EPSPs was 0.28, whereas the average coupling ratio of 30 natural EPSPs was 0.41 ± 0.04.

From the bimodal experimental rise time distribution of EPSPs recorded at the soma of one neuron (Fig. 7 *B*), we assumed that one input to each neuron was located symmetrically on each side of the electrical synapse. The exact location of both presynaptic chemical inputs was determined by simulating the somatic rise time of EPSPs in terms of the electrotonic distance along the coupled neurites. Since the rise time dependence of the input position comes from the ℓ/λ coefficient, its value was adjusted in the model to calculate the input locations which produced EPSPs with somatic rise times of 5.6 and 9.6 ms. The ℓ/λ coefficient which gave the best fits was 0.45 ± 0.7, and the distance from the electrical synapse to the chemical inputs was 0.15 ± 0.05 ℓ, or 7.5 μm, assuming that $\ell = 50$ μm ($n = 7$ neurons). These results were similar if the rise time distributions of EPSPs were obtained using a physiological (1.8 mM) calcium concentration (Fig. 7 *B*) or if the presynaptic release

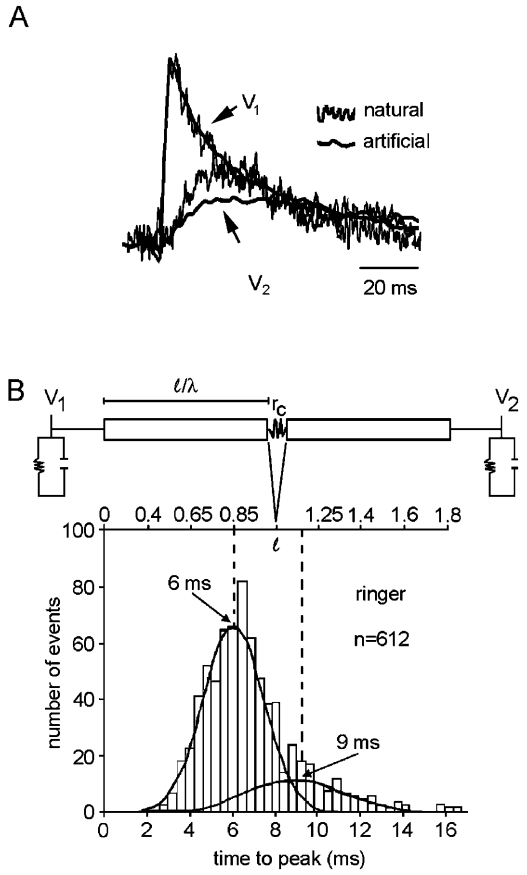

FIGURE 7 Location of synaptic inputs. (*A*) The coupling ratio of artificial EPSPs produced in the soma (V_1) was smaller than the coupling ratio of natural EPSPs produced in one of the neurons showing that synaptic inputs were in the coupled neurites. (*B*) The model simulations were combined with the rise time distributions of EPSPs to predict the locations of the inputs along the coupled neurites. The rise time distributions of natural EPSPs recorded in the soma of one of the neurons (V_1) had two Gaussian peaks, suggesting two major input domains. By adjusting the ℓ/λ coefficient, the model translated the rise time distributions to equivalent electrotonic distances equidistant from the electrical synapse (*top scale*). The distance from the electrical synapse to the presynaptic chemical inputs was 0.15 ℓ (7.5 μm).

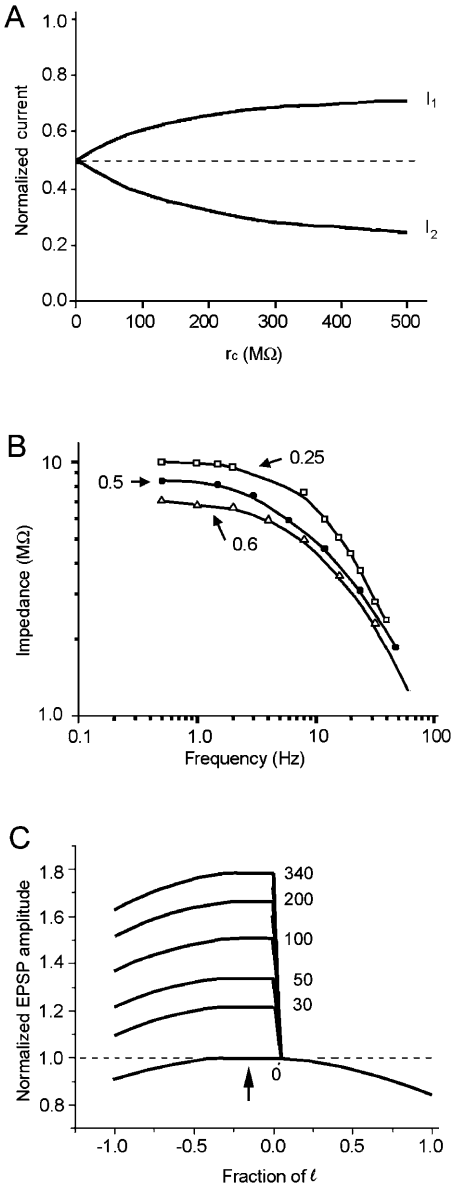

FIGURE 8 Modulation of the EPSP amplified by electrical synapses. (*A*) Model predictions for the distribution of synaptic current on both sides of the electrical synapse as a function of the coupling resistance value. I_1 is the current in the driving neurite, and I_2 is the current in the coupled neurite. The asymmetry of the curves is due to the location of the presynaptic chemical input at 0.15 ℓ from the electrical synapse. Currents were normalized to those when the $r_c = 0$ MΩ. (*B*) Reciprocal relationship between the frequency-dependent impedance ($Z = V_1/I$) and the steady-state coupling ratio. Symbols represent experimental measurements taken from neurons with coupling ratios of 0.25, 0.50, and 0.6. The lines were traced freehand after the data points were obtained. (*C*) The amplitude of EPSPs (*arrow*) depended on the value of the coupling resistance. The horizontal axis is the distance along both coupled neurites, assuming that ($\ell = 0$) is the electrical synapse and that the somata are connected at distances $\ell = -1$ (driving neuron) and $\ell = 1$ (coupled neuron). The origin of EPSPs was at a distance $\ell = -0.15$ (*arrow*). The amplitude of EPSPs was normalized to that when $r_c = 0$. The amplitude of the EPSP produced in the coupled neurite from current produced in the driving neurite was the same for all of the coupling resistance values. The decay of EPSPs along the neurites had the same Gaussian shape for all of the coupling resistance values.

probability was reduced by using a solution with 1.0 mM calcium and 2.0 mM magnesium during the recordings (not shown).

Electrical coupling modulates the amplitude of EPSPs

Electrical coupling of the neurites affected two variables that determined the amplitude of EPSPs. One was the distribution of chemically induced synaptic currents in both coupled neurites, and the second was their impedance. The distribution of synaptic currents as a function of the value of r_c was calculated by the model (Fig. 8 *A*). As expected, when $r_c = 0$ MΩ, both neurites behaved as a continuous cable, and

current spread equally well toward both somata. For this reason, the current values at different r_c values were normalized to those calculated when $r_c = 0$. The asymmetry of the curves in Fig. 8 *A* was due to the input location at 0.15 ℓ from the electrical synapse.

The effect of electrical coupling on the impedance ($Z = V/I$) is shown in Fig. 8 *B*. The plot of the frequency-dependent impedance was obtained experimentally by injection of sine wave currents to pairs of neurons with steady-state coupling values of 0.25, 0.5, and 0.6. As expected, the impedance was inversely proportional to the steady-state coupling ratio, and directly proportional to the estimated r_c values, which were 62, 100, and 250 MΩ, respectively. Since by Ohm's law the amplitude of the EPSPs in the driving neurite was dependent on the product of the impedance and the current, increasing the r_c value produced larger EPSPs. Again, the values presented in Fig. 8 *C* were normalized to those predicted when $r_c = 0$ MΩ. As can be seen, the EPSP amplitude was 80% larger when the coupling resistance was 340 MΩ. Fig. 8 *C* also shows that the EPSP amplitude decayed along the neurites in a Gaussian manner independently on the r_c value because of the frequency dependence of EPSP passive spread (Jack et al., 1975).

Interestingly, our model predicted that the amplitude of EPSPs produced in the coupled neurite by the arrival of synaptic current from the driving neurite was the same at all values of r_c (Fig. 8 *C*). This was because at high r_c values, the impedance increase compensated for the reduction of the amount of current leaking through the coupling resistance. Simulations of EPSPs arriving at the somata of both coupled dendrites at different coupling resistance values and placing the inputs at both different distances from the electrical synapse of one neuron are shown in Fig. 9.

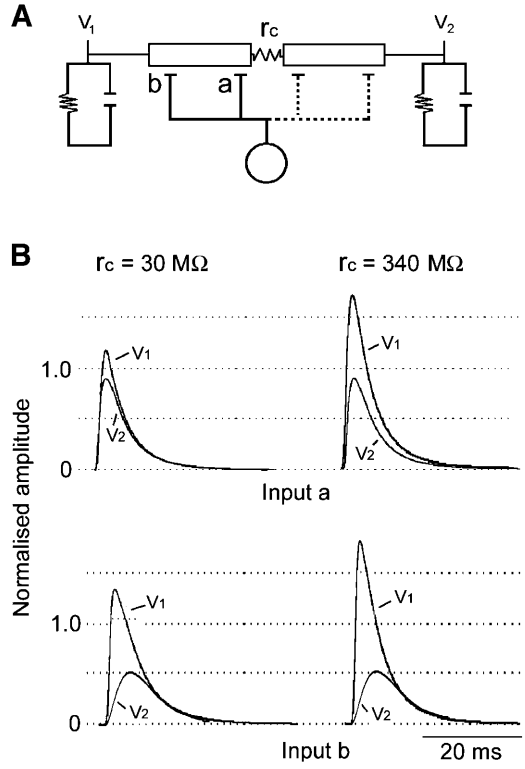

FIGURE 9 Effect of coupling resistance and input location on EPSPs arriving at both somata. (*A*) Diagram of the circuit with two presynaptic inputs at 0.15 and 0.85 ℓ from the electrical synapse. (*B*) Simulations of EPSPs produced by Input a (*top*) and Input b (*bottom*), arriving at both somata are superimposed. The coupling resistance values used were 30 (*left*) and 340 MΩ (*right*). The amplitudes were normalized to those of EPSPs produced when $r_c = 0$ MΩ.

DISCUSSION

We studied how electrical coupling affects the integration of EPSPs. As our main finding we predicted that electrical coupling modulates the amplitude of EPSPs in the driving neurite. Our results were highly dependent on the cytoarchitecture of the neurons. The location of presynaptic inputs near the electrical synapse and the 0.5 value of the ℓ/λ coefficient of the coupled neurites allowed synaptic currents produced in either neurite to arrive at the soma of both neurons. In the driving neurite, the EPSP amplitude was dependent on the coupling resistance value. In the coupled neurite, the amplitude of EPSPs produced by synaptic currents arriving from the driving dendrite was constant at all coupling resistance values.

Possible functional significance

Retzius neurons generate action potentials from the summation of EPSPs produced at their coupled neurites (Fig. 1). Therefore, the amplitude modulation of EPSPs in the driving neurite by the electrical synapse could influence the firing frequency of the neurons, because summation of larger EPSPs produced at high r_c values would increase the probability of reaching the threshold for action potentials. In the coupled neuron, the constant-amplitude EPSPs arriving from the driving neuron regardless of the coupling resistance value guarantees that each EPSP produced in the coupled neurite may take part in the integration process. In addition, currents produced by action potentials in the primary axon back-propagate to the coupled neuron through the electrical synapse (Fig. 1 *D*). Therefore, this combination of chemical and electrical synapses with purely passive membrane properties allows several effects on integration.

Other evidence contributes to the understanding of how EPSPs are integrated by these neurons: 45 of the neurites make contact with the coupled neuron, suggesting a similar number of electrical synapses. Since several, if not all, of them may have chemical inputs, the dominance of unitary events in the amplitude distributions of EPSPs (F. F. De-Miguel and E. García-Perez, unpublished) makes it probabilistically very unlikely that double or triple synaptic events are produced at individual neurites. As a consequence of this,

the summation of unitary EPSPs arriving from different coupled neurites must occur at the primary axon. An advantage of this design would be a reduction of nonlinear effects produced by temporal summation in the same neurite (Magee, 2000).

It is remarkable that the cytoarchitecture of the coupled neurites is designed to function as a single unit. For example, the 0.5 ℓ/λ coefficient of a single coupled neurite is half of those of mammalian or lamprey motoneurons (Christensen and Teubl, 1979; Gustafsson and Pinter, 1984; Bras et al., 1987), lateral geniculate neurons of the cat (Bloomfield et al., 1987), guinea pig cerebellar Purkinje cells (Rapp et al., 1994), or electrically coupled photoreceptor cells in the turtle retina (Detwiler and Hodgkin, 1979). In Retzius neurons this small coefficient allows pairs of coupled neurites to act in series, integrating EPSPs produced by both neurons, regardless on the value of the coupling resistance.

Another aspect of the cytoarchitecture that is relevant from the functional point of view concerns the large areas of the soma and axons as compared with those of the fine neurites. Retzius neurons take advantage of their soma surface to release large amounts of serotonin upon high-frequency trains of impulses (Trueta et al., 2003). The large membrane area of the soma and primary axon as compared with that of the neurites produces a very low somatodendritic conductance coefficient ($\rho \approx 10^{-2}$ to 10^{-1}; see the Supplementary Material). This relationship is opposite to that of vertebrate neurons, in which the surface area of the soma is only a fraction of that of the dendrites (Rall, 1959). The low ρ value suggests that the specific membrane resistance of the soma and primary axon is larger than that of the neurites and explains why, despite such morphology, it is possible to record from the soma the EPSPs produced in the small neurites. This coefficient also suggests that EPSPs recorded at the soma are attenuated as they arrive at the primary axon.

Possible general significance

An increasing amount of evidence from electrophysiological experiments and from the expression patterns of gap junction proteins indicates that a large proportion of central neurons of vertebrates and invertebrates are electrically coupled (for a review, see Dermietzel and Spray, 1993). Some of the functions of electrical synapses, such as the mediation of fast behavioral responses and the synchronization of groups of neurons, are common to invertebrates and vertebrates, including mammals (Furshpan and Potter, 1959; Lin and Faber, 1988; Christie et al., 1989; Valiante et al., 1995; Ishimatsu and Williams, 1996; Mann-Metzer and Yarom, 1999; Galarreta and Hestrin, 1999; Gibson et al., 1999), and so are their modulatory capabilities (Colombaioni and Brunelli, 1988; DeVries and Schwartz, 1989). In addition, the coexistence of chemical and electrical synapses is well-established in the vertebrate nervous systems (Martin and Pilar, 1963). Therefore, even though electrical coupling in invertebrates is mediated by a different set of proteins (Phelan et al., 1998), it is likely that EPSP spread through electrical synapses may also be conserved as part of the integrative mechanisms of neurons of higher animals. Therefore, our prediction of an amplitude modulation of synaptic potentials by electrical synapses may be a first approximation to the understanding of a common mechanism of synaptic integration in the nervous system.

SUPPLEMENTARY MATERIAL

An online supplement to this article can be found by visiting BJ Online at http://www.biophysj.org.

We are greatly indebted to Mr. Bruno Mendez for his invaluable technical assistance in our experiments.

The Computing and Microscopy Units at our Institute provided continuous support during this project. E.G.P. was supported by Consejo Nacional de Ciencia y Tecnología (CONACYT) and Dirección general de estudios de posgrado. M.V.C. and E.G.P. received complementary fellowships from a Human Frontiers Science Program grant (RG-162/98) to F.F.M. Human Frontiers Science Program (RG-162/98), CONACYT (1285-N9204), and Programa de apoyo a proyectos de investigación e inovación tecnológica (IN-207593) grants to F.F.M. gave support to this project.

REFERENCES

Auerbach, A. A., and M. V. L. Bennett. 1969. A rectifying electrotonic synapse in the central nervous system of a vertebrate. *J. Gen. Physiol.* 53:211–237.

Baker, R., and R. Llinás, R.1971. Electrotonic coupling between neurones in the rat mesencephalic nucleus. *J. Physiol. (London)* 212:45–63.

Bennett, M. V. L., E. Aljure, Y. Nakajima, and G. D. Pappas. 1963. Electrotonic junctions between teleost spinal neurons: electrophysiology and ultrastructure. *Science.* 141:262–264.

Bloomfield, S. A., J. E. Hamos, and S. M. Sherman. 1987. Passive cable properties and morphological correlates of neurones in the lateral geniculate nucleus of the cat. *J. Physiol.* 383:653–692.

Bras, H., P. Gogan, and S. Tyc-Dumont. 1987. The dendrites of single brain-stem motoneurons intracellularly labeled with horseradish peroxidase in the cat. Morphological and electrical differences. *Neuroscience.* 22:947–970.

Burrell, B. D., C. L. Sahley, and K. J. Muller. 2001. Non-associative learning and serotonin induce similar bi-directional changes in excitability of a neuron critical for learning in the medicinal leech. *J. Neurosci.* 21:1401–1412.

Christensen, B. N., and W. Teubl. 1979. Estimates of cable parameters in lamprey spinal cord neurons. *J. Physiol.* 297:299–318.

Christie, M. J., J. T. Williams, and R. A. North. 1989. Electrical coupling synchronizes subthreshold activity in locus coeruleus neurons in vitro from neonatal rats. *J. Neurosci.* 9:3584–3589.

Colombaioni, L., and M. Brunelli. 1988. Neurotransmitter-induced modulation of an electrotonic synapse in the CNS of *Hirudo medicinalis*. *Exp. Biol.* 47:139–144.

De-Miguel, F. F., M. Vargas-Caballero, and E. Garcia-Perez. 2001. Spread of potentials through electrical synapsis in Retzius neurones of the leech. *J. Exp. Biol.* 204:3241–3250.

Dermietzel, R., and D. C. Spray. 1993. Gap junctions in the brain: where, what type, how many and why? *Trends Neurosci.* 16:186–192.

Detwiler, P. B., and A. L. Hodgkin. 1979. Electrical coupling between cones in turtle retina. *J. Physiol.* 291:75–100.

DeVries, S. H., and E. A. Schwartz. 1989. Modulation of an electrical synapse between solitary pairs of catfish horizontal cells by dopamine and second messengers. *J. Physiol.* 414:351–375.

Dietzel, I. D., P. Drapeau, and J. G. Nicholls. 1986. Voltage dependence of 5-hydroxytryptamine release at a synapse between identified leech neurones in culture. *J. Physiol.* 372:191–205.

Eckert, R. 1963. Electrical interaction of paired ganglion cells in the leech. *J. Gen. Physiol.* 46:573–587.

Furshpan, E. J., and D. D. Potter. 1959. Transmission at the giant motor synapses of the crayfish. *J. Physiol.* 145:289–325.

Galarreta, M., and S. Hestrin. 1999. A network of fast-spiking cells in the neocortex connected by electrical synapses. *Nature.* 402:72–75.

Galarreta, M., and S. Hestrin. 2001. Spike transmission and synchrony detection in networks of GABAergic interneurons. *Science.* 292:2295–2299.

García, U., S. Grumbacher-Reinert, R. Bookman, and H. Reuter. 1990. Distributions of Na^+ and K^+ currents in soma, axons and growth cones of leech Retzius neurones in culture. *J. Exp. Biol.* 150:1–17.

Gibson, J. R., M. Beierlein, and B. W. Connors. 1999. Two networks of electrically coupled inhibitory neurons in neocortex. *Nature.* 402:75–79.

Gustafsson, B., and M. J. Pinter. 1984. Relations among passive electrical properties of lumbar α-motoneurones of the cat. *J. Physiol.* 356:401–431.

Hagiwara, S., and H. Morita. 1962. Electrotonic transmission between two nerve cells in the leech ganglion. *J. Neurophysiol.* 25:721–731.

Henderson, L. 1983. The role of 5-hydroxytryptamine as a transmitter between identified leech neurons in culture. *J. Physiol.* 339:311–326.

Ishimatsu, M., and J. T. Williams. 1996. Synchronous activity in locus coeruleus results from dendritic interactions in pericoerulear regions. *J. Neurosci.* 16:5196–5204.

Jack, J. J., D. Noble, and R. W. Tsien. 1975. Electric Current Flow in Excitable Cells. Clarendon Press, Oxford.

Korn, H., C. Sotelo, and F. Crepel. 1973. Electronic coupling between neurons in the rat lateral vestibular nucleus. *Exp. Brain Res.* 16:255–275.

Kristan, W. B. 1982. Sensory and motor neurons responsible for the local bending response in leeches. *J. Exp. Biol.* 96:161–180.

Lent, C. M. 1973. Retzius cells from segmental ganglia of four species of leeches: comparative neuronal geometry. *Comp. Biochem. Physiol. A.* 44:35–40.

Lin, J. W., and D. Faber. 1988. Synaptic transmission mediated by single club endings on the goldfish Mauthner cell. I. Characteristics of electrotonic and chemical postsynaptic potentials. *J. Neurosci.* 8:1302–1312.

Llinás, R., R. Baker, and C. Sotelo. 1974. Electrotonic coupling between neurons in cat inferior olive. *J. Neurophysiol.* 37:560–571.

Lockery, S. R., and W. B. Kristan. 1990. Distributed processing of sensory information in the leech. II. Identification of interneurones contributing to the local bending reflex. *J. Neurosci.* 10:1816–1829.

Macagno, E. R., K. J. Muller, W. B. Kristan, S. A. Deriemer, R. Stewart, and B. Granzow. 1981. Mapping of neuronal contacts with intracellular injection of horseradish peroxidase and Lucifer yellow in combination. *Brain Res.* 217:143–149.

Magee, J. 2000. Dendritic integration of excitatory synaptic input. *Nat. Neurosci.* 1:181–190.

Mann-Metzer, P., and Y. Yarom. 1999. Electrotonic coupling interacts with intrinsic properties to generate synchronized activity in cerebellar networks of inhibitory interneurons. *J. Neurosci.* 19:3298–3306.

Marder, E., and J. S. Eisen. 1984. Electrically coupled pacemaker neurons respond differently to the same physiological inputs and neurotransmitters. *J. Neurophysiol.* 51:1362–1374.

Martin, A. R., and G. Pilar. 1963. Dual mode of synaptic transmission in the avian ciliary ganglion. *J. Physiol.* 168:443–463.

Mason, A., and L. D. Leake. 1978. Morphology of leech Retzius cells demonstrated by intracellular injection of horseradish peroxidase. *Comp. Biochem. Physiol. A.* 61:213–216.

McMahon, D. G. 1994. Modulation of synaptic transmission in zebrafish retinal horizontal cells. *J. Neurosci.* 14:1722–1734.

Muller, K. J., and U. J. McMahan. 1976. The shapes of sensory and motor neurones and the distribution of their synapses in ganglia of the leech: a study using intracellular injection of horseradish peroxidase. *Proc. R. Soc. Lond. B Biol. Sci.* 194:481–499.

Nicholls, J. G., and D. Purves. 1972. A comparison of chemical and electrical synaptic transmission between single sensory cells and a motoneurone in the central nervous system of the leech. *J. Physiol.* 225:637–656.

Nusbaum, M. P., and B. W. Kristan. 1986. Swim initiation in the leech by serotonin-containing interneurones, cells 21 and 61. *J. Exp. Biol.* 122: 277–302.

Phelan, P., J. P. Bacon, J. A. Davies, L. A. Stebbings, M. G. Toodmand, L. Avery, R. A. Baines, T. M. Barnes, C. Ford, S. Hekimi, R. Lee, J. E. Shaw, T. A. Starich, K. D. Curtin, Y. Sun, and R. J. Wyaman. 1998. Innexins: a family of invertebrate gap-junction proteins. *Trends Genet.* 14:348–349.

Rall, W. 1959. Branching dendritic trees and motoneuron membrane resistivity. *Exp. Neurol.* 1:491–527.

Rapp, M., I. Segev, and Y. Yarom. 1994. Physiology, morphology and detailed passive models of guinea-pig cerebellar Purkinje cells. *J. Physiol.* 474:101–118.

Rela, L., and L. Szczupak. 2003. Coactivation of motoneurons regulated by a network combining electrical and chemical synapses. *J. Neurosci.* 23:682–692.

Ross, W. N., H. Aréchiga, and J. G. Nicholls. 1987. Optical recording of calcium and voltage transients following impulses in cell bodies and processes of identified leech neurons in culture. *J. Neurosci.* 7:3877–3887.

Schmalbruch, H., and H. Jahnsen. 1981. Gap junctions on CA3 pyramidal cells of guinea pig hippocampus shown by freeze-fracture. *Brain Res.* 217:175–178.

Stewart, W. W. 1978. Intracellular marking of neurons with a highly fluorescent naphthalimide dye. *Cell.* 14:741–759.

Szabadics, J., A. Lorincz, and G. Tamas. 2001. Beta and gamma frequency synchronization by dendritic gabaergic synapses and gap junctions in a network of cortical interneurons. *J. Neurosci.* 21:5824–5831.

Tamas, G., E. H. Buhl, A. Lorincz, and P. Somogyi. 2000. Proximally targeted GABAergic synapses and gap junctions synchronize cortical interneurons. *Nat. Neurosci.* 3:366–371.

Trueta, C., B, Mendez, and F. F. De-Miguel. 2003. Somatic exocytosis of serotonin mediated by L-type calcium channels in cultured leech neurones. *J. Physiol.* 547(Pt 2):405–416.

Valiante, T. A., J. L. Pérez-Velázquez, S. S. Jahromi, and P. L. Carlen. 1995. Coupling potentials in CA1 neurons during calcium-free-induced field burst activity. *J. Neurosci.* 15:6946–6956.

Willard, A. L. 1981. Effects of serotonin on the generation of the motor program for swimming by the medical leech. *J. Neurosci.* 1:936–944.

Yang, J., and K. M. Chapman. 1983. Frequency domain analysis of electrotonic coupling between leech Retzius cells. *Biophys. J.* 44:91–99.